Maximize the Properties of thermoelectric in $LaCoO_3$ by Sr Doping

[1]Dron Mishra, [2]Mukesh Patidar, [3]Varsha Malviya, [4]Sachin Singh Chauhan, [5]Daxa Vekariya

[1, 3] Department of Physics, Renaissance University, Indore (Madhya Pradesh), India

[2, 5] Department of Computer Science & Engineering, Parul Institute of Engineering and Technology, (Parul University), Vadodara (Gujarat), India

[4]Choithram college of professional studies, Indore (Madhya Pradesh) India

[1]dron.mishra@yahoo.com, [2]mukesh.omppatidar@gmail.com, [3]varsha.a2612@gmail.com, [4]sachinrajsingh2012@gmail.com, [5]daxa.vekariya18436@paruluniversity.ac.in

ABSTRACT: $La_{1-x}Sr_xCoO_3$ ceramics thermoelectric properties are analyzed hypothetically, it is watched that most extreme esteem of figure of justify ZT (= $S^2\sigma T/\kappa$) by the substitution of Sr in $La_{1-x}Sr_xCoO_3$ at x = 0.02. The Hamiltonian demonstrate is utilized for numerical result, the phonon commitment assessed by the unwinding time estimation for thermoelectric control and warm conductivity. It is located that substitution of La with Sr in $LaCoO_3$ reduces in Seebeck coefficient and advancement in electrical conductivity recognizably. The enhancement in ZT in $La_{0.7}Sr_{0.3}CoO_3$ (LSCO) at 800K which is 5 times more than of $LaCoO_3$. The hypothetical values are in great assentation with the exploratory values.

Keywords: Thermal conductivity, ZT, $La_{0.7}Sr_{0.3}CoO_3$ (LSCO), Coefficient of Seebeck, $LaCoO_3$, Thermoelectric (TE).

1. Introduction

$LaCoO_3$, Seebeck coefficient, Warm conductivity, ZT justify & Ceramics Presentation Thermoelectric (TE) vitality transformation may be a promising innovation for era of electrical control in terms of warm recuperation. The figure of justify decide vitality change productivity of materials, spoken to as ZT = $S^2\sigma T/k$ where S is Seebeck coefficient, k is warm conductivity, s is electrical conductivity and T is Temperature. Great thermoelectric fabric with a tall figure of justify ZT ought to have moo warm conductivity and tall electrical conductivity, Seebeck coefficient. Thermoelectric execution of customary TE compounds can be effectively get oxidized or deteriorated in discuss at tall temperatures constraining its application [1-5].

TE fabric Cobalt oxides are utilized since of its expansive electric conductivity and Seebeck coefficient [6]. They appear a solid related electron framework with La particles displaying an vitality level decline of electronic states, which is consider at moo temperature as beginning of huge Seebeck coefficient. Rhombohedra misshaped perovskite structure of Lanthanum cobalt oxide gives a ordinary illustration of warm helped turn state move of trivalent cobalt. It is conceivable alter its sign by reasonable substitution to progress the Seebeck coefficient esteem. For the arrangement of thermoelectric devices the not at all like layered oxides and LaCoO3 which may not require a lumbering strategy of epitaxial development. Substitution of Sr is productively progressed the thermoelectric execution of ceramics LaCoO3.

The typical sintering strategy and strong state response were create the ceramic test $La_{1-x}Sr_xCoO_3$, and the impact La substitution with Sr particles was inspected by the assessment of Seebeck coefficient and electrical conductivity [7-8]. It was found that the figure of justify was essentially upgraded [1].

Thus, when Sr is substituted in $La_{1-x}Sr_xCoO_3$, the concentration in number gaps increases and the Seebeck coefficient falls. Either gaps are created, i.e., La^{2+} is oxidized, or oxygen vacancies are produced to compensate for the surplus negative charge age presented by Sr^{2+} doping in $LaCoO_3$ [2, 9]. The Seebeck decreases when raising the temperature as the turn state moves.

When temperatures go above 327^0C, the transport component contributing to the Seebeck coefficient is overwhelmed by newly introduced frame gaps and turn state move wraps-up caused by doping. Hence, it decreases to a lower constant value at high temperature. At ambient temperature, the un-doped $LaCoO_3$ gives a steadily negative Seebeck coefficient. In any case, the Seebeck coefficient went from negative to positive with very little Sr substitution [1].

After that, Sr-doped $LaCoO_3$ thermoelectric characteristics are most likely shown. The Hamiltonian-display is utilized as a numerical result, and the phonon commitment is determined from the estimation of the unwinding time for thermoelectric power and thermal conductivity [10–12]. The shown Hamiltonians generate phonons, surrenders, electrons, and grain boundaries. To suit the available numbers from the tests, the electron contribution to thermal conductivity and thermoelectric power is assessed.

2. The Model

The Hamilton model used to calculate the theoretical values is described in [10-12].

$$H = \Sigma\ \varepsilon_k\ c_k^+ c_k\ +\Sigma\ \omega_q d_q^+ d_q\ + D_p \sum_{k,q}^{q} \left[\frac{\hbar}{2\rho\omega_q}\right]^{1/2} c_{k+q}^+ c_k \left(d_q\ +\ d_{-q}^+\right)$$

$$+\ \frac{M_i}{2N} \sum_{q_1, q_2} e^{i(q_1+q_2)\eta} \left[\frac{\hbar\omega_{q1}\,\hbar\omega_{q2}}{4}\right]^{1/2} \left(d_{q_1}\ -\ d_{-q_1}^+\right)\left(d_{q_2}\ -\ d_{-q_2}^+\right) \quad (1)$$

The first two terms refer to the electron as a carrier and the phonon excitation. The third and fourth terms define the phonon-carrier and phonon-impurity interactions, respectively. The last term relates to the phonon-phonon interaction. The notations c (c+) and d (d+) are electron and phonon creation (annihilation) operators. Additionally, εk is the free energy of the electron, q denotes the phonon frequency corresponding to the wave vector q, and Dp is the deformation potential constant. Mi is the relative difference in the masses of ions taken [(M"-M)/M"], N being the total number of cells, ri the mass density of the ions, and ri the defect location.

Kubo's equation can be employed to calculate thermal conductivity according to the Hamiltonian model (Equation 1). Under continuous approximation, the lattice thermal conduction is given as follows:

$$\kappa_{ph} = \frac{k_B \hbar^2}{2\pi^2 v_s} \int_0^{\omega_D} d\omega \omega^2 \tau(\omega)(\beta\omega)^2 \frac{e^{\beta\omega}}{(e^{\beta\omega}-1)^2}. \tag{2}$$

There, vs is the sound speed, k_B is Boltzmann's constant, ωD is the Debye frequency, and β = η/kBT. The imaginary part of the phonon energy determines relaxation time, which was calculated at the base of different interactions under weak interaction conditions. This is how one writes relaxation time.

$$1/\tau(\omega) = 2\left|\mathrm{Im}\, P(\omega/v_S, \omega)\right| \tag{3}$$

$$= 1/\tau_{ph-d} + 1/\tau_{ph-e} + 1/\tau_{ph-gb} + 1/\tau_{ph-ph}, \tag{4}$$

Rates with extended periods of relaxation are described as:

$$\tau_{ph-d}^{-1}(\omega) = (P_d / k_B^3)\omega^4 \hbar^3, \tag{5}$$

$$\tau_{ph-e}^{-1}(\omega) = P_e \omega n_F(\Delta), \tag{6}$$

$$\tau_{ph-gb}^{-1}(\omega) = P_{gb} v_S / L, \tag{7}$$

$$\tau_{ph-ph}^{-1}(\omega) = P_p \left(T\omega\hbar / k_B\right)^3. \tag{8}$$

In which nF signifies the Fermi-Dirac distribution function L as size of the sample and the Δ is gap function. The relaxation times of phonons scattering of defects, of carriers, and of particles are τph-d, τph-e, τph-gb, τph-ph respectively.

$$S = \frac{8\pi^2 kB^2}{3eh^2}(\pi / 3n)^{2/3} m * T \tag{9}$$

$$1 / ZT = k / S^2 \sigma T \tag{10}$$

3. Results and Discussion

The Seebeck coefficient ZT merit calculations for the thermal conductivity model mentioned above were carried out and contrasted with the existing experimental results. I got it. The following figure compares the computed ZT value, Seebeck coefficient, and thermal conductivity with the experimental results. In Fig. 1, Fig. 2 and Fig. 3 represent the analysis result of Seebeck coefficient, Thermal conductivity and ZT varies with temperature for different

doping concentration, experimental data (Red Circles) respectively. The Table 1 represents Seebeck coefficient data.

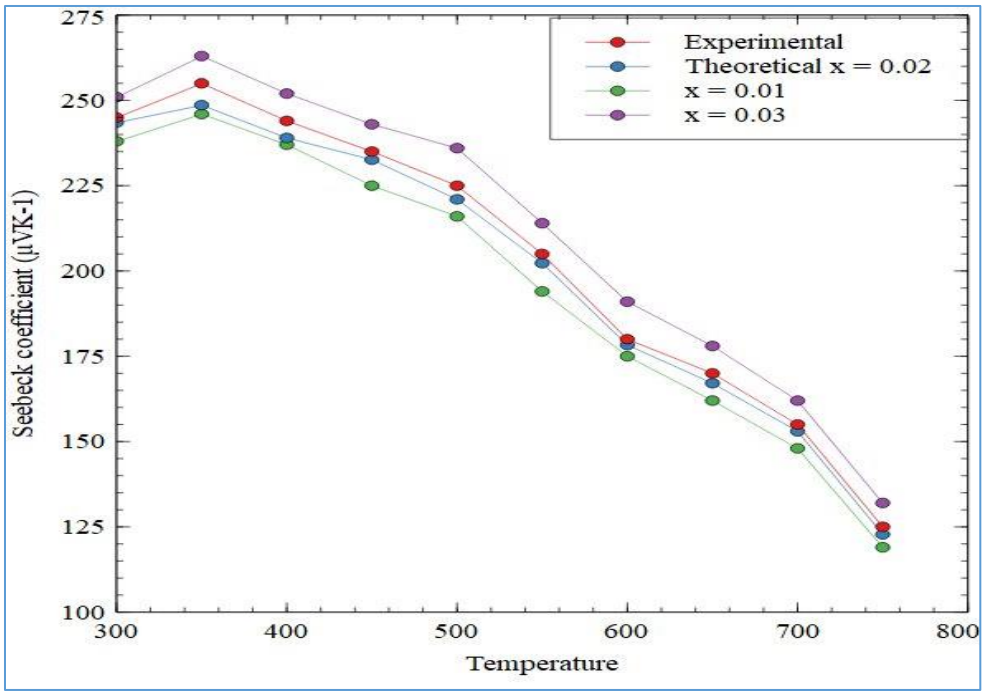

Fig. 1 Seebeck coefficient varies with temperature for different doping concentration. Experimental data (Red Circles)

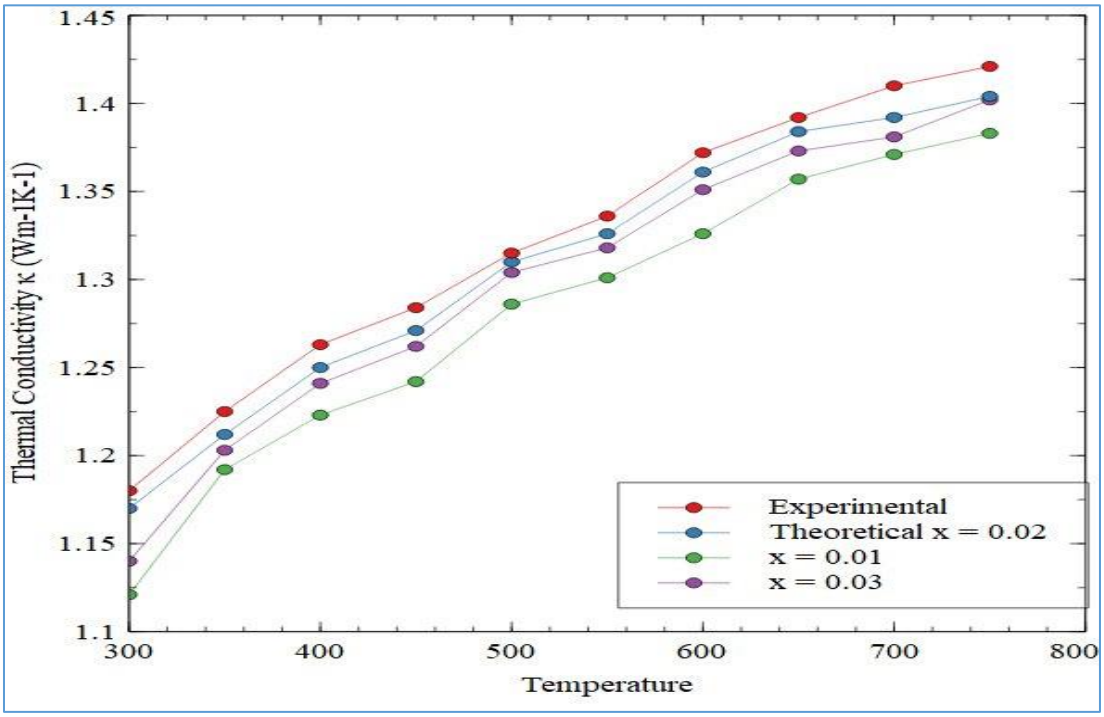

Fig. 2 Thermal conductivity varies with temperature for different doping concentration

Table 1: Seebeck Coefficient Data Table

Temperature (K)	Experimental (μV/K)	Theoretical x=0.02 (μV/K)	x=0.01 (μV/K)
300	250	250	240
400	240	235	230
500	215	210	205
600	185	180	175
700	125	125	120

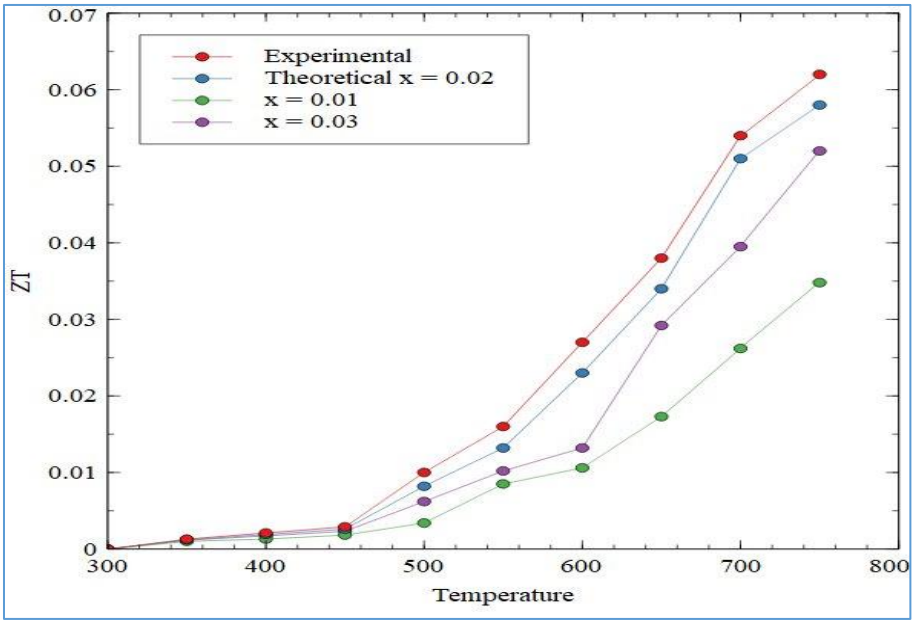

Fig. 3 ZT varies with temperature for different doping concentration

4. CONCLUSION

It is located that Sr substitution in $LaCoO_3$ enhance the electrical conduction, but coefficient of seebeck is reduced. The result in improvement in ZT in $La_{0.7}Sr_{0.3}CoO_3$ at 800K which is 5 times more than of $LaCoO_3$. It show that substituted element is effective to compress the grain growth of ceramic $LaCoO_3$, which can decrease the thermal conductivity. Therefore we obtained in the composition of $La_{1-x}Sr_xCoO_3$ with maximum of 0.02 at 800K enhance the ZT value. The theoretical parameter evaluated by using the Hamiltonian are best agreement with the experimental parameter.

REFERENCES

1. J. Han, Y. Song, X. Liu, and F. Wang, "Sintering behavior and thermoelectric properties of LaCoO3 ceramics with Bi2O3–B2O3–SiO2 as a sintering aid," *The Royal Society of Chemistry*, vol. 4, no. 94, 2024. DOI: 10.1039/C4RA06735E.
2. A. Kumar, D. Sivaprahasam, and A. D. Thakur, "Improvement in thermoelectric properties in (1-x) LaCoO3 / (x) La0.7Sr0.3CoO3 composite," *Materials Chemistry and Physics*, vol. 269, 2021, Art. no. 124750.
3. F. Li and J. Li, "Effect of Ni substitution on electrical and thermoelectric properties of LaCoO3 ceramics," *Ceramics International*, vol. 37, pp. 105–110, 2011.
4. D. Enescu, "Thermoelectric Energy Harvesting: Basic Principles and Applications," *Green Energy Advances*, IntechOpen, Feb. 20, 2019. DOI: 10.5772/intechopen.83495.

5. H. Cheng, X. J. Xu, H. H. Hng, and J. Ma, "Characterization of Al-doped ZnO thermoelectric materials prepared by RF plasma powder processing and hot press sintering," *Ceramics International*, vol. 35, pp. 3067–3072, 2009.
6. U. Deepika Shanubhogue, A. Pal, A. Rao, et al., "Tuning optical and thermoelectric properties of LaCoO3: Partial substitution of La by isovalent Gd," *Journal of Alloys and Compounds*, vol. 941, Art. no. 168987, Apr. 2023. DOI: 10.1016/j.jallcom.2023.168987.
7. Y. Wang, Y. Sui, J. Cheng, X. J. Wang, J. P. Miao, Z. G. Liu, Z. N. Qian, and W. H. Su, "High temperature transport and thermoelectric properties of Ag-substituted Ca3CO4O9+delta system," *Journal of Alloys and Compounds*, vol. 448, pp. 1–5, 2008.
8. R. Funahashi and S. Urata, "Fabrication and application of an oxide thermoelectric system," *International Journal of Applied Ceramic Technology*, vol. 4, pp. 297–307, 2007.
9. M. Patidar and N. Gupta, "Efficient design and implementation of a robust coplanar crossover and multilayer hybrid full adder–subtractor using QCA technology," *Journal of Supercomputing*, vol. 77, pp. 7893–7915, 2021. DOI: 10.1007/s11227-020-03592-5.
10. A. Kumar, D. Sivaprahasam, and A. D. Thakur, "Improved thermoelectric properties in (1-x)LaCoO3/(x)La0.7Sr0.3CoO3 composite," *Materials Chemistry and Physics*, vol. 269, Art. no. 124750, Sep. 2021. DOI: 10.1016/j.matchemphys.2021.124750.
11. Y. F. Zhang, J. X. Zhang, and Q. M. Lu, "Synthesis of highly textured Ca3Co4O9 ceramics by spark plasma sintering," *Ceramics International*, vol. 33, pp. 1305–1308, 2007.
12. R. Robert, L. Bocher, B. Sipos, M. Dobeli, and A. Weidenkaff, "Ni-doped cobaltates as potential materials for high temperature solar thermoelectric converters," *Progress in Solid State Chemistry*, vol. 35, pp. 447–455, 2007.
13. R. Robert, L. Bocher, M. Trottmann, A. Reller, and A. Weidenkaff, "Synthesis and high-temperature thermoelectric properties of Ni and Ti substituted LaCoO3," *Journal of Solid State Chemistry*, vol. 179, pp. 3893–3899, 2006.
14. M. Patidar and N. Gupta, "Efficient design and simulation of novel exclusive-OR gate based on nanoelectronics using quantum-dot cellular automata," in *Lecture Notes in Electrical Engineering*, vol. 476, Springer, Singapore, 2019. DOI: 10.1007/978-981-10-8234-4_48.
15. A. Kumar, et al., "Thermoelectric Properties of (1 − x) LaCoO3.(x)La0.95Sr0.05CoO3 composite," *Materials Research Express*, vol. 6, Art. no. 055502, 2019. DOI: 10.1088/2053-1591/aade73.
16. T. He, J. Z. Chen, T. G. Calvarese, and M. A. Subramanian, "Thermoelectric properties of La(1—x)A(x)CoO(3) (A = Pb, Na)," *Solid State Sciences*, vol. 8, pp. 467–469, 2006.
17. K. Choudhary, D. Mishra, U. Sharma, and N. Kaurav, "Enhancement in specific heat by nanocrystallization: Softening of phonon frequencies mechanism," *International Journal of Modern Physics B*, vol. 31, Art. no. 1850027, 2017.
18. K. Choudhary, N. Kaurav, and S. Ghosh, "Optimization of thermoelectric properties by Cu substitution in LaCoO3 ceramics," *International Journal of Modern Physics B*, vol. 28, Art. no. 1450065, 2014.
19. U. Sharma and D. Mishra, "Interpretation of thermal conductivity of ceramic oxides," in *AIP Conf. Proc.*, vol. 2100, Art. no. 020042, 2019.
20. A. Doi, et al., "Positive temperature coefficient of the thermal conductivity above room temperature in a perovskite cobaltite," *Science and Technology of Advanced Materials*, vol. 23, no. 1, 2022. DOI: 10.1080/14686996.2022.2149035.
21. M. Patidar and N. Gupta, "An efficient design of edge-triggered synchronous memory element using quantum dot cellular automata with optimized energy dissipation," *Journal of Computational Electronics*, vol. 19, pp. 529–542, 2020. DOI: 10.1007/s10825-020-01457-x.